Marine Pollution Bulletin 129 (2018) 729–739

Contents lists available at ScienceDirect

Marine Pollution Bulletin

journal homepage: www.elsevier.com/locate/marpolbul

Aragonite saturation state in a tropical coastal embayment dominated by phytoplankton blooms (Guanabara Bay – Brazil)

Luiz C. Cotovicz Jr[a,c,*], Bastiaan A. Knoppers[a], Nilva Brandini[b], Dominique Poirier[c], Suzan J. Costa Santos[a], Gwenaël Abril[a,c,d]

[a] Departamento de Geoquímica, Laboratório de Biogeoquímica Marinha, Universidade Federal Fluminense, Outeiro São João Batista s/n, 24020015 Niterói, RJ, Brazil
[b] Programa de Pós-graduação em Geografia, Laboratório de Ciências do Mar, Instituto de Geografia, Desenvolvimento e Meio Ambiente, Universidade Federal de Alagoas, 57072900 Maceió, AL, Brazil
[c] Laboratoire Environnements et Paléoenvironnements Océaniques et Continentaux (EPOC), CNRS, Université de Bordeaux, Allée Geoffroy Saint-Hilaire, 33615 Pessac Cedex, France
[d] Laboratoire d'Océanographie et du Climat: Expérimentations et Analyses Numériques (LOCEAN), Centre IRD France Nord, 32 avenue Henri Varagnat, 93143 Bondy Cedex, France

ARTICLE INFO

Keywords:
Carbonate chemistry
Coastal eutrophication
Coastal acidification
Phytoplankton blooms

ABSTRACT

The dynamics of the aragonite saturation state (Ω_{arag}) were investigated in the eutrophic coastal waters of Guanabara Bay (RJ-Brazil). Large phytoplankton blooms stimulated by a high nutrient enrichment promoted the production of organic matter with strong uptake of dissolved inorganic carbon (DIC) in surface waters, lowering the concentrations of dissolved carbon dioxide (CO_{2aq}), and increasing the pH, Ω_{arag} and carbonate ion (CO_3^{2-}), especially during summer. The increase of Ω_{arag} related to biological activity was also evident comparing the negative relationship between the Ω_{arag} and the apparent utilization of oxygen (AOU), with a very close behavior between the slopes of the linear regression and the Redfield ratio. The lowest values of Ω_{arag} were found at low-buffered waters in regions that receive direct discharges from domestic effluents and polluted rivers, with episodic evidences of corrosive waters ($\Omega_{arag} < 1$). This study showed that the eutrophication controlled the variations of Ω_{arag} in Guanabara Bay.

1. Introduction

The human activities are altering the biogeochemical cycles of essential elements at unprecedented levels (Howarth et al., 2011). The burning of fossil fuels and land-use-change activities have been altering the global cycle of carbon by increasing the emissions of carbon dioxide (CO_2) to the atmosphere (IPCC, 2013). The global average atmospheric CO_2 has increased from 277 ppmv in 1750 to approximately 400 ppmv in 2015, and, together with the increase of other greenhouse gases, are driving important environmental changes (Gattuso et al., 2015; Le Quéré et al., 2016). Taking account the global CO_2 budget calculated for the period between 2006 and 2015, approximately 43% of the total anthropogenic CO_2 emissions remained in the atmosphere (4.5 ± 0.1 Gt C yr^{-1}), whereas the oceans sequestered approximately 25% (2.6 ± 0.5 Gt C yr^{-1}) (Le Quéré et al., 2016).

When the CO_2 dissolves in the water, a series of reactions and processes takes place, producing non-ionic and ionic compounds (Millero, 2007; Dickson, 2010). The dissolved CO_2 (CO_{2aq}) is the dominant carbon dioxide species when the pH is lower than 5, however, at higher pH, the CO_{2aq} ionizes to form bicarbonate (HCO_3^-) and carbonate (CO_3^{2-}) anions (Dickson, 2010). The sum of CO_{2aq}, HCO_3^- and CO_3^{2-} comprehends the dissolved inorganic carbon (DIC). The CO_{2aq} is proportional to the partial pressure of CO_2 (pCO_2) in the water. When CO_2 hydrates and/or ionizes, it releases hydrogen ions (H^+), lowering the pH. Therefore, the absorption of CO_2 by the oceans results in a decrease in pH and CO_3^{2-} concentrations. Low pH values can inhibit and/or hinder the ability of many marine organisms to form calcium carbonate ($CaCO_3$) skeletons and shells (Gattuso et al., 2015). In extreme scenarios, this can promote dissolution of $CaCO_3$ because the water becomes undersatuated with respect to $CaCO_3$ minerals (Feely et al., 2008; Zhai et al., 2015). However, studies also showed that some organisms could be resistant to ocean acidification effects. A study conducted in an Arctic coastal region showed that the taxonomic composition of zooplankton species remained unaffected by changes in pCO_2/pH (Aberle et al., 2013). In addition, the abundance of some species of zooplankton from the Bay of Bengal were found to be

* Corresponding author at: Departamento de Geoquímica, Laboratório de Biogeoquímica Marinha, Universidade Federal Fluminense, Outeiro São João Batista s/n, 24020015 Niterói, RJ, Brazil.
E-mail address: lccjunior@id.uff.br (L.C. Cotovicz).

http://dx.doi.org/10.1016/j.marpolbul.2017.10.064
Received 28 September 2017; Received in revised form 17 October 2017; Accepted 22 October 2017
Available online 06 November 2017
0025-326X/ © 2017 Elsevier Ltd. All rights reserved.

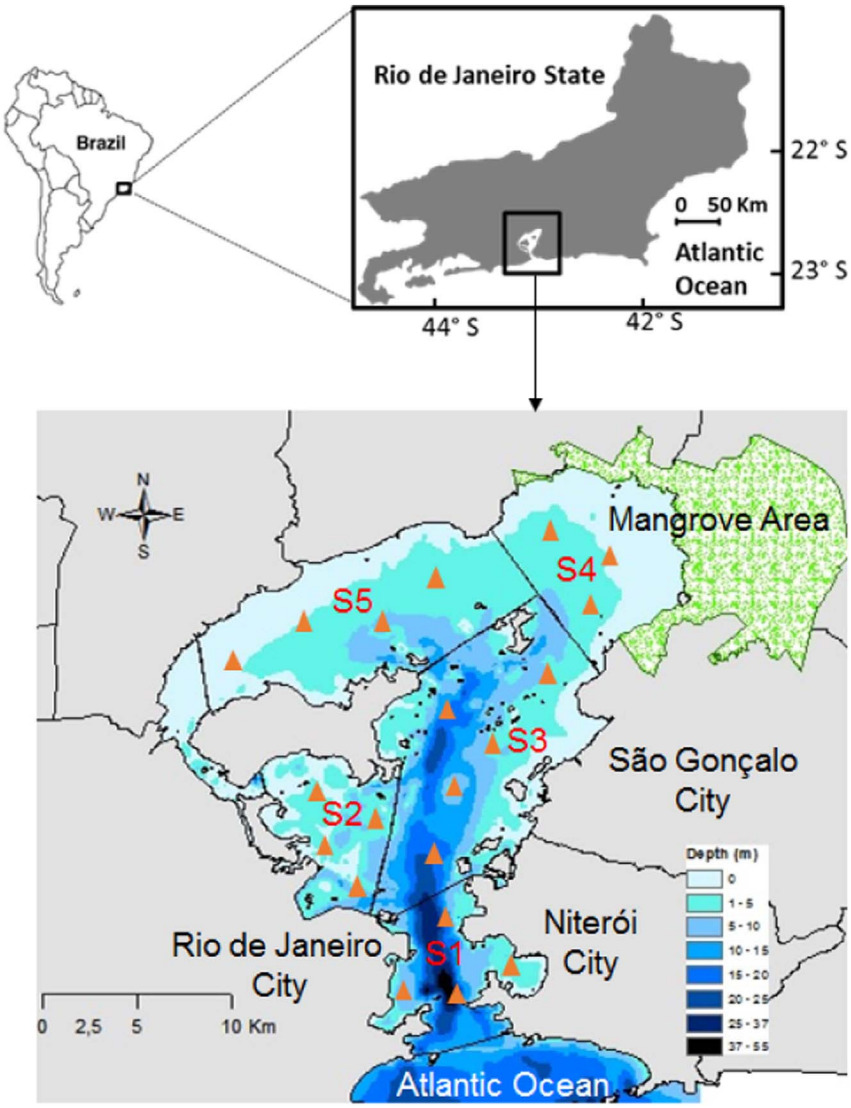

Fig. 1. Map of Guanabara Bay. The bay was divided into five sectors (S1 to S5). The red triangles represent the sampling stations. (For interpretation of the references to color in this figure legend, the reader is referred to the web version of this article.)

significantly higher under elevated CO_2 levels (Biswas et al., 2012). In this way, the effects of ocean acidification seem to be specific considering different organisms and ecosystems, with winners and losers under high CO_2 conditions.

The $CaCO_3$ saturation state of seawater (Ω) with respect to a particular $CaCO_3$ mineral can be calculated to infer the tendency of precipitation or dissolution (Dickson, 2010). The aragonite is usually the principal form of $CaCO_3$ in shallow waters and is approximately 50% more soluble than calcite (Morse et al., 2007; Mucci, 1983). This mineral is essential to many phytoplanktonic and benthonic species (Gattuso et al., 2015). Due to this, the studies of saturation state of aragonite (Ω_{arag}) have received attention in the last 10 years, especially in coastal environments (Feely et al., 2010; Zhai et al., 2015; Hu et al., 2017; Xue et al., 2017). The Ω_{arag} can be defined by the formula:

$$\Omega_{ararg} = [Ca^{2+}]\,[CO_3^{2-}]/K_{sp}(arag)$$

where, $[Ca^{2+}]$ $[CO_3^{2-}]$ is the observed ion product between calcium and carbonate concentration and K_{sp}(arag) is the solubility product of aragonite in seawater. $\Omega_{arag} > 1$ indicates that the precipitation of aragonite is favored and the minerals are stable; $\Omega_{arag} < 1$ indicates that aragonite minerals are unstable in the water and can dissolve; $\Omega_{arag} = 1$ indicates equilibrium between precipitation and dissolution. The ocean acidification is commonly referred to the modifications in marine carbonate chemistry, driven by the increase of atmospheric CO_2, with the increase of CO_{2aq}, and decrease of pH, CO_3^2, Ω and the buffer capacity of seawater (Doney et al., 2009). This problem has recently taken attention from the scientific community due to projected threats that could affect marine species, communities and ecosystems (Doney et al., 2009; Kroeker et al., 2010; Gattuso et al., 2015).

In coastal waters, the variations of carbonate parameters are also strongly affected by the mixing processes between freshwater and seawater, upwelling and eutrophication, and the controlling mechanisms of Ω_{arag} are more complex than in the open ocean (Salisbury et al., 2008; Cai et al., 2011; Duarte et al., 2013; Zhai et al., 2015; Xue et al., 2016; Hu et al., 2017). The coastal ocean responds differently from the open ocean to CO_2 inputs, and can be more vulnerable to negative effects of ocean and coastal acidification (Zhai et al., 2015). This vulnerability was described in some coastal zones due to the influence of metabolic processes adding high CO_2 into the waters, and associated with low values of pH and $\Omega_{arag} < 1$ in sub-surface and bottom waters (Feely et al., 2008, 2010; Cai et al., 2011; Zhai et al., 2015). This occurs because the anthropogenic inputs of organic matter and nutrients associated with strong eutrophication processes have fueled massive algal blooms, which deplete the oxygen and release CO_2 when the organic matter is respired (Cai et al., 2011; Sunda and Cai, 2012; Wallace et al., 2014). Previous studies on eutrophication in coastal waters have been focused on the investigation of the nutrient, chlorophyll *a* (Chl *a*) and oxygen levels (hypoxia and anoxia) in the waters (Nixon, 1995; Bricker

et al., 2003; Rabalais et al., 2009; Ferreira et al., 2011). However, recent studies have been reported that eutrophication can also contributes to the coastal acidification (Provoost et al., 2010; Cai et al., 2011; Wallace et al., 2014). It is important to point, therefore, that the ocean acidification in open ocean waters is driven by external loading of CO_2 (atmospheric inputs), whereas in coastal zones this loading is mainly driven by internal processes related to microbial respiration (Wallace et al., 2014). Moreover, it must be keep in mind that the coastal eutrophication can also drawdown the levels of aquatic CO_2 due to the stimulation of primary production, with uptake of atmospheric CO_2 (Borges and Gypens, 2010; Cotovicz et al., 2015; Kubo et al., 2017).

The carbonate system responses in face to these CO_2 changes (uptake and/or emission) driven by eutrophication remains largely unknown and especially overlooked in ecosystems located at tropical regions. Hereby, we present the spatio-temporal results of Ω_{arag} and buffer capacity in the productive waters of Guanabara Bay (RJ, Brazil), a highly eutrophic and densely populated tropical estuary. Our results showed that phytoplankton blooms control the values of Ω_{arag} and pH, which were positively correlated with the concentrations of Chl *a*, dissolved oxygen (DO), and water temperature. The results suggest that the variation of pH related to eutrophication is more important than the changes in carbonate chemistry predicted by the increase of atmospheric CO_2 concentrations.

2. Material and methods

2.1. Study area

Guanabara Bay (22°41–22°58 S and 43°02–43°18 W) is a marine-dominated estuary located at the Southeastern coast of Brazil (Fig. 1). This estuary is the second largest bay in Brazil, occupying an area of 384 km^2. It is one extreme example of a polluted bay where about 16 millions of inhabitants live on its surroundings and watershed (Fistarol et al., 2015). The drainage basin of Guanabara Bay covers an area of 4081 km^2, which is composed of 16 municipalities, 50 rivers and streams (Kjerfve et al., 1997). However, only 6 rivers abide to > 80% of the total mean annual freshwater discharge, which was estimated at about 125 $m^3 s^{-1}$ (Kjerfve et al., 1997). This relative low input of freshwater compared to the water volume of Guanabara Bay contributes to salinities normally higher than 25 (Kjerfve et al., 1997; Cotovicz et al., 2015). The climate pattern in the region presents two distinct periods: a warm and rainy summer (October to Abril) and a dry and colder winter (May to September).

The sewage and water treatment plants are very limited in the watershed (Fistarol et al., 2015), causing discharge of large amounts of both domestic and industrial effluents "*in natura*" into the bay at about 25$m^3 s^{-1}$ (Kjerfve et al., 1997). These large inputs of effluents translate in a high eutrophication process. The organic carbon load to the sediment increased 10 times in the last 50 years (Carreira et al., 2002), and the sedimentation increased up to 14-times over the last 50 years (Godoy et al., 2012). Large phytoplankton blooms dominate the surface waters, with high contribution of autochthonous source to the particulate and sedimentary organic carbon (Carreira et al., 2002; Kalas et al., 2009). In addition, the bay is a strong annual sink of CO_2 due to the high uptake of inorganic carbon by large phytoplankton blooms (Cotovicz et al., 2015).

The driving phytoplankton assemblages of Guanabara Bay are typical for eutrophic to hypertrophic systems, largely dominated by nanoplankton (flagellates and diatoms, < 20 μm) and filamentous cyanobacteria (Valentin et al., 1999; Santos et al., 2007; Villac and Tenenbaum, 2010). The most prominent species of phytoplankton in Guanabara Bay are the dinoflagellate *Scrippsiella trochoidea* and diatoms from the *Skeletonema costatum* complex (Villac and Tenenbaum, 2010). Considering the relative number of taxa within various taxonomic groups, the diatoms represents 62%, dinoflagelates 42%, cyanobacterias 2.8%, euglenophyceans 1.5%, and others 1.5% (Villac and Tenenbaum, 2010).

Despite the fact that this system is heavily impacted by anthropogenic activities, there are important calcifying organisms that could be found at the benthic environment, including calcareous benthic foraminifera and ostracod (Vilela et al., 2003; Clemente et al., 2014). Benthic foraminifera and ostracod answer to changes in environmental parameters and have important uses in ecology and paleoecology studies (Vilela et al., 2003; Murray, 2006). The benthic foraminifera assemblage found in Guanabara presented weak and fragile tests, with various types of deformities (Vilela et al., 2003; Clemente et al., 2014). Morphological variations in the benthic foraminifera tests have been related to a combination of several parameters, including the carbonate solubility (Boltovskoy et al., 1991). There are also species of echinoderms, as sea urchins and starfishes (Meniconi et al., 2012), which needs $CaCO_3$ to construct the skeletons (Miles et al., 2007). In addition, there are important species of mollusks and crustaceans found in consolidate substrates of Guanabara Bay (Meniconi et al., 2012), including oysters and mussels that biomineralizes $CaCO_3$ to build the shells (Fitzer et al., 2016). In general, the diversity of mollusks and crustaceans follows the concentrations of dissolved oxygen in bottom waters of Guanabara Bay (Meniconi et al., 2012).

Due to the spatial heterogeneity in the hydrological and geomorphological characteristics, and the differential anthropogenic occupation of the watershed, we compartmentalized the bay in five domains (sectors 1, 2, 3, 4 and 5; Fig. 1), which are well described in Cotovicz et al. (2015, 2016).

2.2. Sampling strategy

Nine sampling campaigns were conducted between 2014 and 2015, with intervals of 30–45 days between each one. The winter period was covered by the months of Apr.2013, Jul.2013, Ago.2013 and Apr.2014, and the summer period was covered by the months of Sep.2013, Oct.2013, Dec.2013 and Jan.2014 represent the summer period. The measurements were conducted with a boat that covered all the sectors of Guanabara Bay (Fig. 1). Along the track of the boat, continuous and discrete samplings were performed. Continuous measurements were carried out for water temperature, salinity, fluorescence, DO and pCO_2. The discrete samples were taken at sub-surface with a Niskin bottle for Chl *a*, pheo-pigments, total alkalinity (TA) and pH. Vertical profiles of temperature, salinity, and DO were performed at all discrete stations with a calibrated multiparameter probe model YSI® 6600 V2.

2.3. Continuous measurements

The continuous measurement system is well described in Cotovicz et al. (2015, 2016). Briefly, a submersible water pump was attached at the side of the boat at a depth of about 0.5 m, providing continuous water flux at 6 L min^{-1}. One part of this water flux (3 L min^{-1}) was directed to an equilibration system to measure the aquatic pCO_2 (marble equilibrator type; Frankignoulle et al., 2001). The marble exchanger consists of an acrylic tube (100 cm long; 8 cm diameter), filled with glass marbles. The marbles increase the exchange area inside the tube to about 1.4 m^2, and reduces the internal tube volume to 0.6 L. The marble equilibrator is connected to a non-dispersive infrared gas detection (NDIR, LI-COR® type LI-820). The air in the equilibrator was dried before passing to the gas analyzer. The LICOR® was calibrated before and after each sampling camping with certified material with air pCO_2 values of 410, 1007 and 5035 ppmv (White Martins Certified Material, RJ, Brazil). The fresh soda lime was used to set the zero and the standard at 1007 ppmv to set the span. The accuracy of pCO_2 measurements was about ± 5 ppmv. The temperature, salinity, fluorescence and DO were measured on-line with a calibrated YSI 6600 V2 multiparameter sonde.

2.4. Laboratory analysis

The water samples were filtered with Whatman GF/F filters and then conditioned (kept in dark and on ice) until the analysis in laboratory. The filters for analysis of Chl *a* and pheo-pigments were kept at − 18 °C in a freezer prior to analysis. The TA measurements were performed with the classical Gran (1952) titration method with an automated titration system (Metler Toledo model T50). The accuracy of this method was ± 7 μmol kg^{-1} and inferred using certified reference material (CRM, A. G. Dickson from Scripps Institution of Oceanography, San Diego). Chl *a* and pheo-pigments were measured in the Whatman GF/F filters following Strickland and Parsons (1972). The pH was measured with a WTW 3310 pH meter equipped with a Sentix 41 electrode, which was calibrated with a three-point standard (pH 4.01, pH 7.00 and pH 10.01) according to the National Institute of Standards and Technology (NIST), before and after each sampling campaign. The precision of the pH measurements was 0.01 (after seven verifications against standards before and after each sampling campaign). The differences between surface and bottom water values in terms of Ω_{arag} and other parameters were only performed at some stations, during the summer period, and during conditions of maximal thermo-haline stratification in sectors 3, 4 and 5. The total number of concomitant surface and bottom water samples was 48, covering the period from Oct.2013 to Feb.2014.

2.5. Calculations

DIC and Ω_{arag} were calculated from pCO_2, TA, seawater temperature, and salinity using the CO2calc 1.2.9 program (Robbins et al., 2010). The dissociation constants for carbonic acid were those proposed by Mehrbach et al. (1973) refitted by Dickson and Millero (1987), the borate acidity constant from Lee et al. (2010), the dissociation constant for the HSO_4^- ion from Dickson (1990) and the CO_2 solubility coefficient of Weiss (1974). The K_{sp} values for aragonite were taken from Mucci (1983) and the concentrations of calcium (Ca^{2+}) were assumed proportional to the salinity variations according to Millero (1979).

To calculate the Ω_{arag} for bottom waters we used the data from pH and TA, using also the CO_2calc 1.2.9 program, and following the same procedures described above. We compare the DIC concentrations calculated from the pCO_2-TA and pH-TA pairs, and the results showed an excellent agreement (slope: 1.008; $R^2 = 0.995$). The slope was not statistically different from 1 ($p = 0.20$) and the intercept was not significantly different from 0 ($p = 0.86$).

The excess of DIC (E-DIC, μmol kg^{-1}) was calculated as follows (Abril et al., 2003):

$$E - DIC = DIC_{in\ situ} - DIC_{equilibrium}$$

where, $DIC_{in\ situ}$ is the concentration of DIC at in situ conditions and $DIC_{equilibrium}$ represents the DIC calculated from the observed TA and pCO_2 values assuming an equilibrium between the aquatic and atmospheric CO_2 concentrations.

The apparent oxygen utilization (AOU, μmol kg^{-1}) was calculated according to Benson and Krause (1984), as following:

$$AOU = DO_{equilibrium} - DO_{in\ situ}$$

where, $DO_{equilibrium}$ represents the value of saturation of oxygen concentration (concentration of oxygen in equilibrium with the atmosphere but corrected according to its *in situ* values of salinity, temperature and pressure) and $DO_{in\ situ}$ represent the concentration of DO at *in situ* conditions.

Various buffer factors can be used to quantify the changes in the buffer capacity of seawater (Frankignoulle, 1994; Egleston et al., 2010). These buffers measure the resistance of seawater to change at a given perturbation, such as increases/decreases of the hydrogen ion concentration (or activity) when DIC changes at constant alkalinity, or vice-versa (Egleston et al., 2010; Wang et al., 2016). In this study, we calculate three buffer factors related to the resistance to change of the pH (β_{DIC}), CO_2 (γ_{DIC}) and Ω (ω_{DIC}), when DIC changes at constant alkalinity (Egleston et al., 2010). These three buffers can be calculated as follow:

$$\beta DIC = -(\partial \ln[H+]/\partial[DIC]) - 1$$

$$\gamma DIC = -(\partial \ln[CO2]/\partial[DIC]) - 1$$

$$\omega DIC = -(\partial \ln \Omega/\partial[DIC]) - 1$$

β_{DIC} quantifies how much hydrogen ion would change in accordance to the change in DIC concentration, γ_{DIC} quantifies how much aqueous CO_2 would change, and ω_{DIC} quantifies how much Ω will change, all considering a constant alkalinity. The ω_{DIC} gives negative values, and henceforth the results we reported as absolute values (ω_{DIC} abs). These buffer factors were calculated using DIC, TA, salinity and temperature data based on the equations derived by Egleston et al. (2010).

2.6. Statistical analysis

We applied the Shapiro-Wilk test to verify the normality of data distributions. As the data presented non-parametric distributions, we used the nonparametric paired Wilcoxon test to compare differences between surface and bottom waters averages. Simple linear regressions were calculated to compare the distributions and correlations between variables. All statistical analysis were based on $\alpha = 0.05$. The statistical tests were performed with the GraphPad Prism 6 program.

3. Results and discussion

3.1. Spatial variations of TA and DIC

Table 1 shows the average, standard deviation, minimum and maximum values for all the water parameters analyzed in this study, separated for the sectors. Fig. 2 shows the seasonal behavior for pH, DIC, CO_{2aq}, HCO_3^-, CO_3^{2-} and Ω_{arag}. Guanabara Bay presents a marked spatio-temporal variability related to the marine carbonate chemistry. It follows the patterns of biological activities related to photoautotrophic primary production and microbial respiration. Due to the high anthropogenic disturbances along the watershed and surrounding areas, Guanabara Bay presented a large variation of freshwater endmembers associated to the multiplicity of point and non-point terrestrial sources, including polluted rivers, sewage discharges and urban runoff (Ribeiro and Kjerfve, 2002; Cotovicz et al., 2015, 2016). Considering this, it was not possible to apply the mixing curves to infer gain or losses of material along the salinity gradient, that is an usual approach to study the carbonate parameters in estuaries and coastal zones (Jiang et al., 2013), especially to investigate the TA and DIC variability.

Even not applying the mixing curves, it was clear that the bay produces considerable amounts of TA especially at the most polluted regions (Fig. 3). The highest deviations above the linear regression between the salinity and TA occurred in sector 2 (maximum TA = 2489 μmol kg^{-1}) and in the sector 5 (maximum TA = 2314 μmol kg^{-1}). These sectors receive high inputs of allochthones sources (domestic effluents) and hypoxia and anoxia events occur (Ribeiro and Kjerfve, 2002; Cotovicz et al., 2015). Diverse processes can contributes with production of anaerobic alkalinity in coastal waters, including ammonification, denitrification and sulphate reduction (Abril and Frankignoulle, 2001; Hu and Cai, 2011). The significantly higher ammonium concentrations in bottom waters compared to surface waters indicates significant diffusion of ammonium from anoxic sediments and confirms the occurrence of anaerobic processes in the sector 2 and parts of sector 4 and 5 (Cotovicz et al., 2016). The other sectors 1, 3 and 4 showed the distributions of TA approaching the conservative behavior, indicating higher dependence to the mixing

Table 1
Mean, standard deviation, minimum and maximum values of the main physico-chemical and carbonate chemistry parameters analyzed in this study in the waters of Guanabara Bay, separated by sectors.

	Sector 1	Sector 2	Sector 3	Sector 4	Sector 5
Temperature	23.8 ± 1.7	25.5 ± 2.2	25.4 ± 2.1	26.8 ± 2.6	26.7 ± 2.2
(°C)	(21.0–29.3)	(22.1–32.4)	(22.1–31.5)	(22.0–32.3)	(22.6–33.9)
Salinity	32.2 ± 2.1	30.3 ± 2.4	29.8 ± 3.0	27.0 ± 4.3	27.2 ± 3.5
	(25.4–34.9)	(17.7–33.7)	(15.1–33.8)	(14.6–33.2)	(16.6–32.9)
pH	8.20 ± 0.16	8.15 ± 0.32	8.35 ± 0.23	8.34 ± 0.29	8.44 ± 0.31
(NBS)	(7.90–8.71)	(7.33–8.96)	(7.88–8.96)	(7.39–9.01)	(7.51–9.23)
DO	103 ± 29	97 ± 59	138 ± 51	142 ± 62	160 ± 69
(%)	(48–221)	(2–263)	(56–357)	(30–361)	(46–370)
Chl-*a*	19.1 ± 22.0	46.2 ± 51.4	57.6 ± 90.0	69.2 ± 60.2	107.7 ± 101.8
($\mu g \cdot L^{-1}$)	(2.0–128.0)	(3.3–212.9)	(1.6–537.2)	(13.1–288.8)	(1.5–822.1)
TA	2240 ± 92	2291 ± 99	2168 ± 177	2045 ± 369	2137 ± 166
($\mu mol \cdot kg^{-1}$)	(1942–2320)	(1890–2489)	(1507–2344)	(1290–2269)	(1479–2314)
DIC	1985 ± 120	2044 ± 268	1847 ± 257	1658 ± 259	1758 ± 264
($\mu mol \cdot kg^{-1}$)	(1720–2127)	(1526–2523)	(1332–2290)	(1095–2118)	(1198–2190)
CO_{2aq}	13.7 ± 4.6	23.5 ± 21.0	10.9 ± 6.8	9.6 ± 10.4	8.7 ± 7.2
($\mu mol \cdot kg^{-1}$)	3.8–20.0	1.7–83.0	1.1–26.2	1.3–53.5	0.6–29.9
HCO_3^-	1770 ± 148	1817 ± 362	1597 ± 322	1404 ± 306	1468 ± 340
($\mu mol \cdot kg^{-1}$)	1347–1952	1048–2385	857–2101	893–1961	669–2046
CO_3^{2-}	189 ± 56	195 ± 132	232 ± 99	233 ± 102	270 ± 112
($\mu mol \cdot kg^{-1}$)	122–361	45–478	105–470	34–476	69–531
Ω_{arag}	3.0 ± 0.9	3.2 ± 2.2	3.8 ± 1.7	3.9 ± 1.7	4.4 ± 1.9
	2.0–5.8	0.8–8.2	1.7–7.9	0.8–7.8	1.1–9.4

processes. Normally, the TA concentrations follow a conservative mixing pattern in estuaries, however non-conservative behavior was also found in other ecosystems (Borges and Abril, 2011).

A marked non-conservative behavior was also observed for the distributions of DIC against salinity (Fig. 4). This indicates that the mixing patterns have minor influence compared to the biological processes of consumption and production of organic matter, since biological production consumes DIC, whereas microbial respiration produces. The most polluted area of the bay (sector 2) receives and produces large amounts of DIC related to the organic carbon inputs sustaining heterotrophic processes (DIC concentrations were highly above the linear regression; Fig. 4). These high DIC concentrations associated to the sewage and urban runoff was related in the highly urbanized Changjiang River Estuary (Zhai et al., 2007). Sectors 3, 5 and partially the sector 4 presented some distributions below the linear regression and related to biological uptake (the minimum value of DIC was 1095 $\mu mol\ kg^{-1}$). As expected, the sector 1, near the bay entrance, showed the lowest variations compared to the regression line indicating that this sector have minor influence from the highly productive mid-upper shallow waters. Previous study showed that the bay is a strong sink of CO_2 (Cotovicz et al., 2015), corroborating the fact that the primary production consumes high amounts of DIC from the water

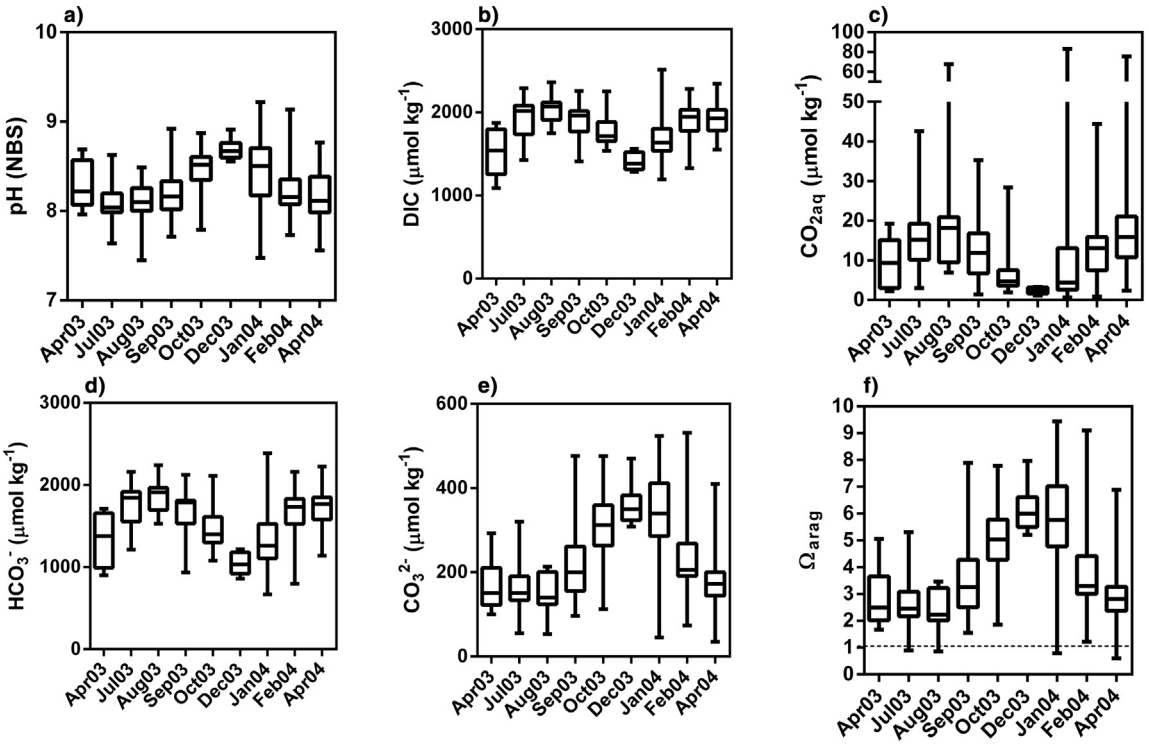

Fig. 2. Box plots (maximum, percentile 75%, median, percentile 25% and minimum) including the annual variations for the following parameters: a) pH; b) DIC; c) CO_{2aq}; d) HCO_3^-; e) CO_3^{2-}; f) Ω_{arag} values for all sampling campaigns.

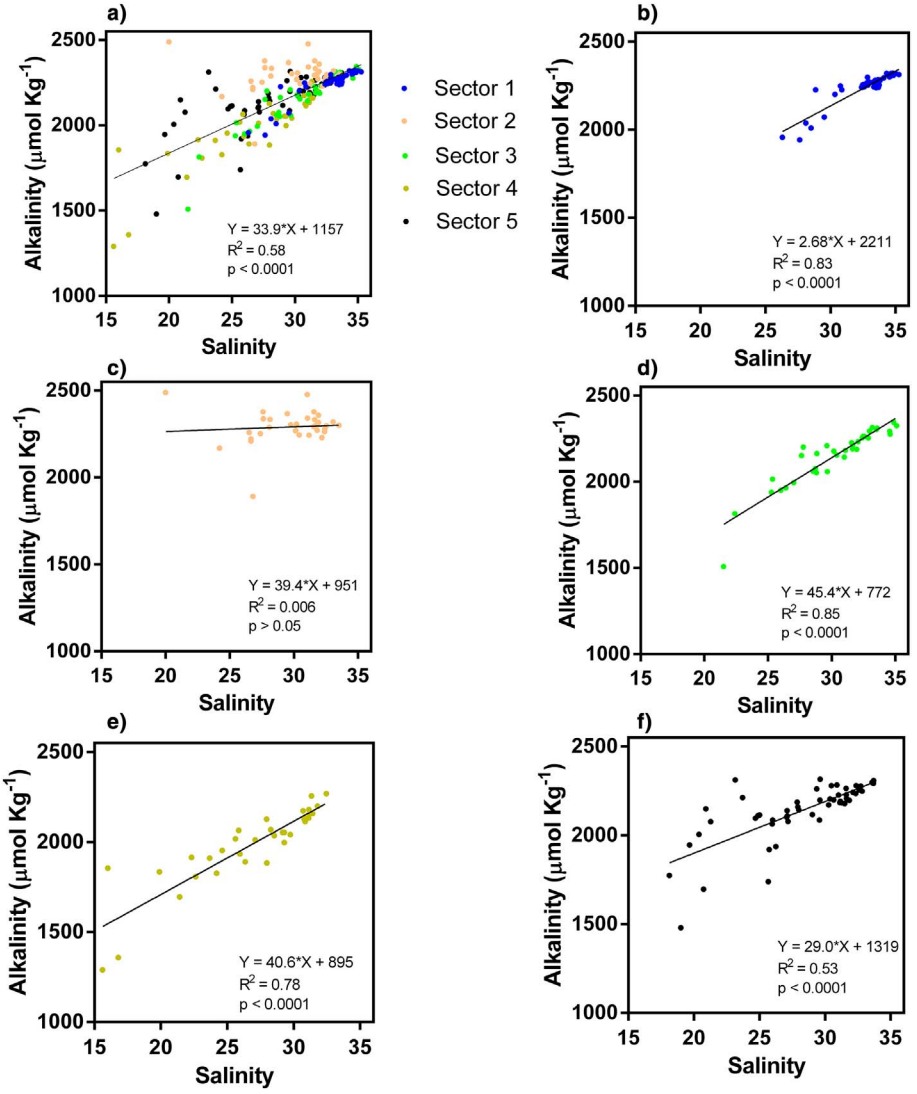

Fig. 3. Relationships between the Ω_{arag} and the total alkalinity concentrations for: a) entire bay; b) sector 1; c) sector 2; d) sector 3; e) sector 4; f) sector 5. The black lines represent the linear regressions.

column, decreasing the levels of CO_{2aq}. This enhanced biological production fueled by nutrient was found in several estuaries, for example, at the Changjiang estuary (Chou et al., 2013) and the Mississippi river plume (Huang et al., 2012), among others. Overall, the DIC concentrations in Guanabara Bay were lower than that found in other coastal embayments, including the subtropical Florida Bay (Zhang and Fischer, 2014), the urbanized Jiaozhou Bay (Zhang et al., 2012) and the temperate Jade Bay at the North Sea (Winde et al., 2014).

3.2. The biological control of Ω_{arag}

The lowest concentrations of DIC were coincident with the highest concentrations of CO_3^{2-} and vice versa (Fig. 1). This can be explained by the speciation of DIC concentrations according to the pH of the seawater (Dickson, 2010), which is in turn controlled by the processes of primary production and respiration. Considering the high DIC scenario (maximum DIC = 2523 µmol kg^{-1}), the high concentrations are driven by strong heterotrophic activities that produces large amounts of CO_{2aq} (maximum CO_{2aq} = 83 µmol kg^{-1}) by the microbial respiration, increasing the HCO_3^- and decreasing the pH, Ω_{arag}, and CO_3^{2-} concentrations. In the case of the low DIC scenario (minimum DIC = 1095 µmol kg^{-1}), the low concentrations are driven by the high rates of primary production, with the uptake of CO_{2aq} (minimum CO_{2aq} = 0.6 µmol kg^{-1}), and increase of pH, CO_3^{2-} and Ω_{arag}. The high DIC scenario can be observed in sector 2, whereas the low DIC scenario is strongest at sector 3, and parts of sectors 4 and 5 under direct influence of phytoplankton blooms.

The strong influence of biological activity over carbonate chemistry for Guanabara Bay can also be noted considering the relationships between pH and AOU, and between Ω_{arag} (normalized at temperature of 25.5 °C; $\Omega_{arag@25.5}$) and AOU (Fig. 5). The Ω_{arag} was normalized to an average temperature to eliminate the thermal effect over Ω_{arag} variations (Xue et al., 2017). Both pH and $\Omega_{arag@25.5}$ were highly negatively correlated to AOU, supporting the hypothesis that high primary production rates contributes with high DO production and increases the $\Omega_{arag@25.5}$. In this way, the variations of pH and $\Omega_{arag@25.5}$ were not related to the increase of atmospheric CO_2 concentrations, but rather related to the phytoplankton autotrophic production. In the graph b of Fig. 5 we included a theoretical line representing the Redfield slope calculated according Xue et al. (2017) (see the figure caption for more details). In this graph, it was possible to see the changes in $\Omega_{arag@25.5}$ only due to biological activity (orange dashed line represents the Redfield slope) and that was very close to the slope of the regression line (black line represents the linear regression). Previous study also showed a good correlation between AOU and *E*-DIC in Guanabara Bay (Winde et al., 2014), where the quotient between CO_2 and O_2 during planktonic primary production and community respiration were close to 1 due to the coupling between gross primary production and total respiration.

The higher influence of primary production was more evident at

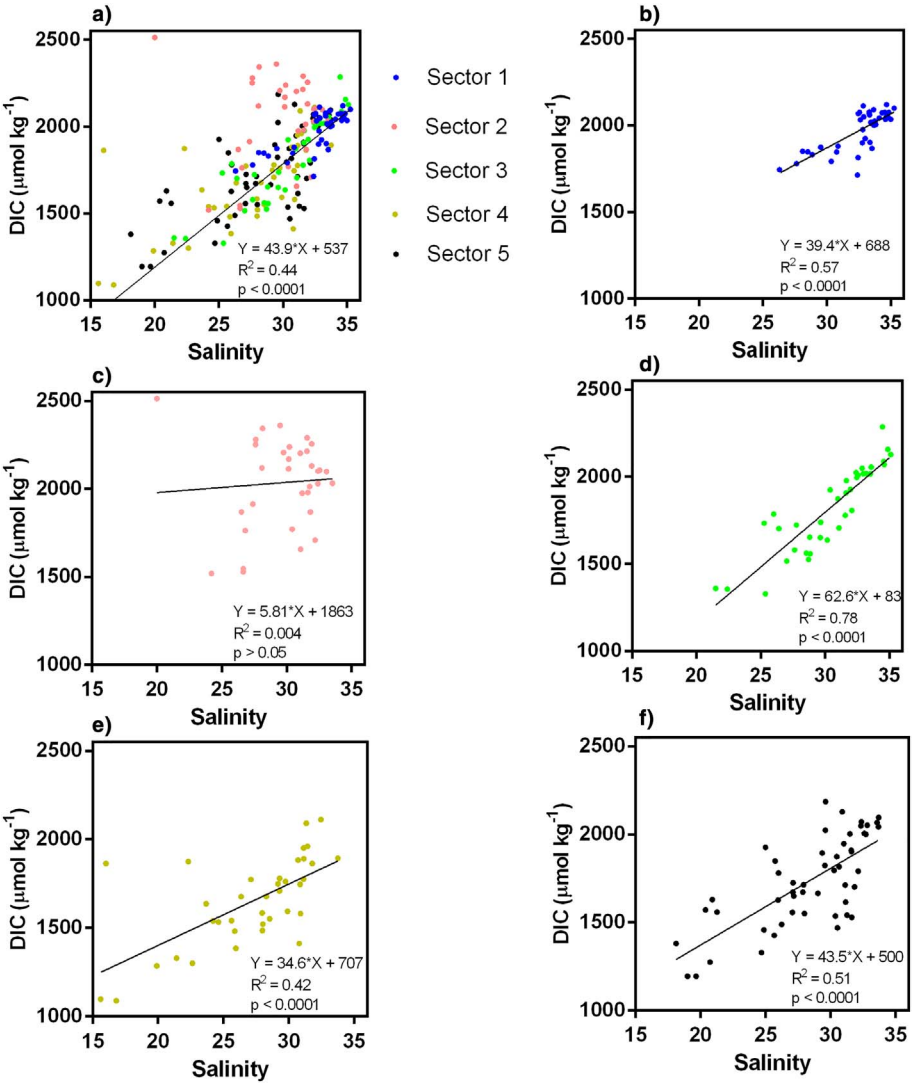

Fig. 4. Relationships between the Ω_{arag} and the DIC concentrations, for: a) entire bay; b) sector 1; c) sector 2; d) sector 3; e) sector 4; f) sector 5. The black lines represent the linear regressions.

inner-mid shallow regions of the bay (sectors 3, 4 and 5), as these regions presented the highest concentrations of Chl *a* (max. = 822 µg L^{-1}), with marked seasonality. During summer, the photosynthetically active radiation is higher, promoting the appearance of thermo-haline stratification and favoring the development of large phytoplankton blooms associated with the high availability of inorganic nutrients (Rebello et al., 1988; Cotovicz et al., 2015). This high primary productivity leads to the uptake of CO_2 (Cotovicz et al., 2015), increasing the pH of the water and consequently increasing the CO_3^{2-} and the Ω_{arag}. The Fig. 6 shows the positive correlations between the $\Omega_{ara@25.5}$ and the seawater temperature, for all the sectors. These graphs indicate that the high water temperature favors the autochthonous primary production in the bay when the CO_2 is converted to biomass. The highest correlation coefficients were in sectors 3 and 5, with values of $R^2 = 0.72$ and $R^2 = 0.63$, respectively, that are the most productive regions of the bay. The lowest values of DO, pH, CO_3^{2-} and Ω_{arag} were observed in winter (Fig. 1). During this period, the primary production is lower and the respiration processes can takes places,

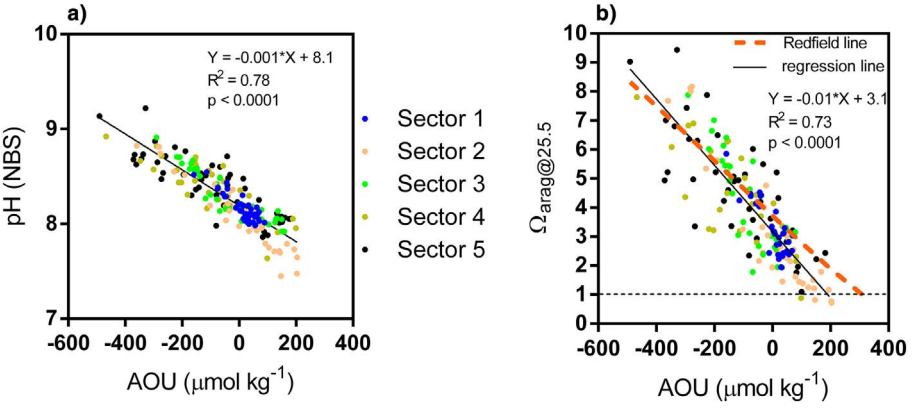

Fig. 5. Relationships between: a) the pH and the AOU concentrations; b) the $\Omega_{arag@25.5}$ and the AOU concentrations. The black lines represent the linear regressions, and the orange line represents the Redfield slope calculated according to Xue et al. (2017). The initial conditions for the calculations were: mean temperature of 25.5 °C, salinity (= 30), TA (= 2096 µmol kg^{-1}) and DIC (= 1328 µmol kg^{-1}), at the minimum AOU of − 490 µmol kg^{-1}. The temperature and salinity were maintained constants, and the TA and DIC changed according to AOU. The changes of biological activity on TA and DIC and thus Ω_{arag} are quantified based on the classic Redfield, that was ΔDIC: ΔTA: ΔDO = − 106:17:138 (Xue et al., 2017). The Ω_{arag} was normalized to the temperature of 25.5 °C ($\Omega_{arag@25.5}$) to eliminate the thermal effect.

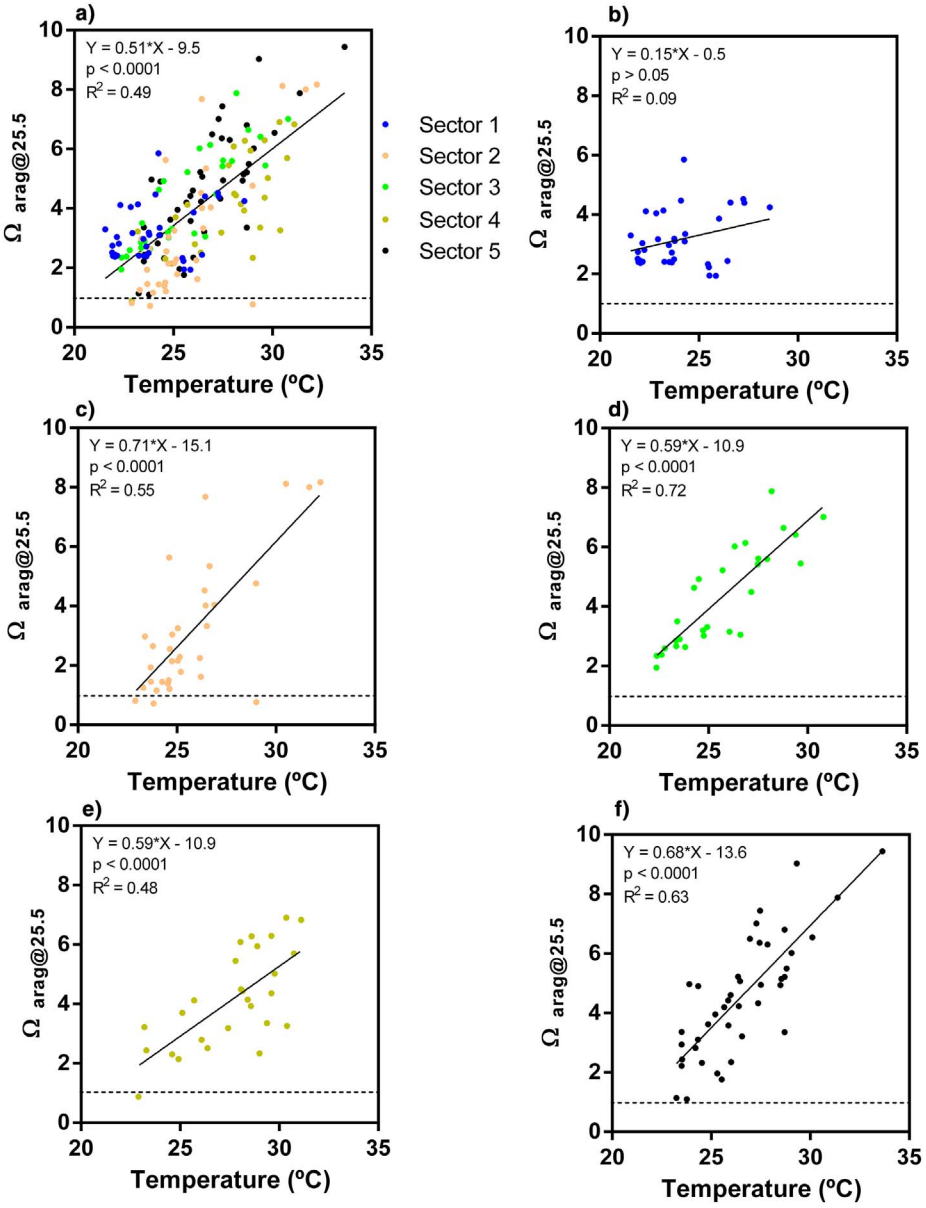

Fig. 6. Relationships between the $\Omega_{arag@25.5}$ and the seawater temperature, for: a) entire bay; b) sector 1; c) sector 2; d) sector 3; e) sector 4; f) sector 5. The black lines represent the linear regressions. The Ω_{arag} was normalized to the temperature of 25.5 °C ($\Omega_{arag@25.5}$) to eliminate the thermal effect.

especially at the locations of the bay that receive direct inputs of nutrients and organic matter. However, it must be highlighted that the phytoplankton blooms are present even during winter, but with low spatial coverage (Cotovicz et al., 2015). The nutrient enrichment in Guanabara Bay contributes with the excess of organic matter produced by the phytoplankton blooms. This is a process well described in other coastal areas worldwide (Diaz and Rosenberg, 2008); however, for Guanabara Bay this process is exacerbated (extreme high concentrations of Chl *a*, that reached a maximum of 822 μg L^{-1}). Previous studies showed that the high productive surface waters can both depressed the CO_{2aq} and elevated the concentrations of Chl *a*, DO, pH, Ω_{arag} and DIC/TA ratio values (Mathis et al., 2010; Wallace et al., 2014; DeJong et al., 2015; Xue et al., 2016; Hu et al., 2017; Cai et al., 2017). As pointed by Borges and Gypens (2010), in eutrophicated coastal waters the increase in pH can be highly significant and can override the signals of carbonate chemistry related to the increase of atmospheric CO_2 concentrations.

The regions of the bay under direct influence of sewage and polluted rivers discharges presented low values of Ω_{arag} during all the year. The values of Ω_{arag} were < 1 in sector 2 and 4 (in two and one time, respectively) and near 1 at sector 5. The values of Ω_{arag} < 1 indicate a possible dissolution of $CaCO_3$ minerals and the organisms that must use the $CaCO_3$ to construct the skeletons could be especially affected (Doney et al., 2009; Gattuso et al., 2015). Our main hypothesis is that the allochthones sources represent the principal inputs of waters with low values of Ω_{arag}. However, the respiration of autochthonous organic matter during the settlement to the bottom waters can also contributes with low values of Ω_{arag}. For example, during summer, bottom samples were taken to investigate the vertical stratification of the water column. The Wilcoxon test showed significant vertical differences of Ω_{arag} with bottom waters presenting lower values than superficial waters (averages of 2.4 ± 0.4 and 4.1 ± 1.4, respectively, Fig. 7). The bottom waters presented also higher values of pCO_2 and lower values of DO, indicating prevalence of microbial respiration below the pycnocline. In this way, during summer, the formation of vertical stratification can prevent the mixing between the ventilated surface waters with the poorly oxygenated bottom waters, contributing with the formation of bottom hypoxia and acidification. The difference between surface and bottom water for Ω_{arag}, pCO_2 and AOU reached a maximum of 4.7, 705 ppmv and 331 μmol kg^{-1}, respectively. This represents a functioning as a "two-layer" system during summer for the highly productive mid-upper regions of the bay, with production processes prevailing

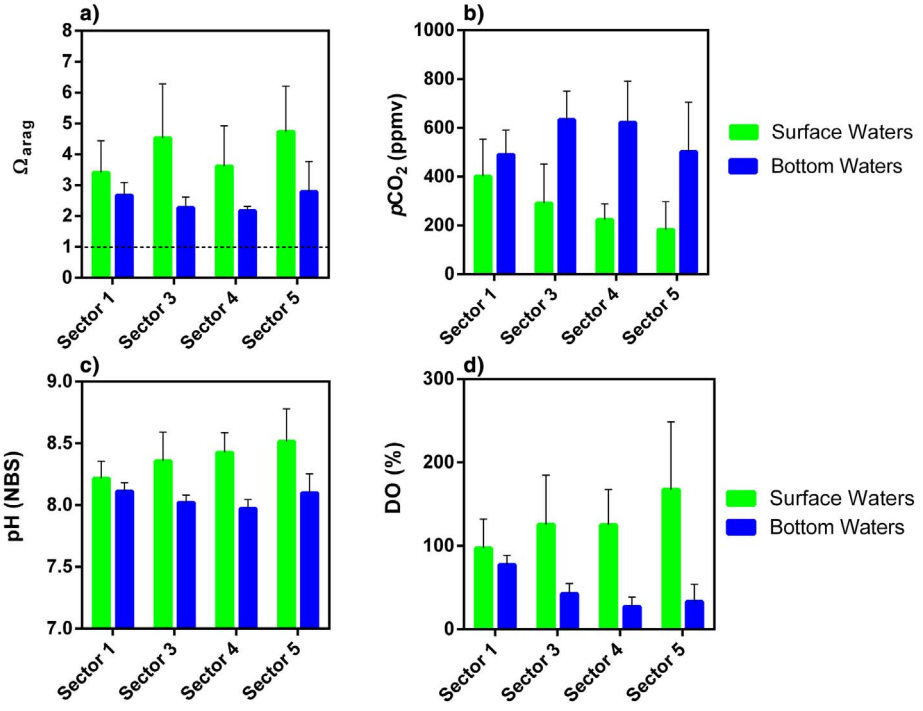

Fig. 7. Comparison between the concentrations of surface and bottom waters for the following parameters: a) Ω_{arag}; b) pCO_2; c) pH; d) DO.

in the upper layer and respiration processes in the lower layer. The development of hypoxia and acidification of subsurface waters due to additional CO_2 was observed in the Gulf of Triest (North Adriatic Sea; Cantoni et al., 2012), Northern Gulf of Mexico (Cai et al., 2011; Sunda and Cai, 2012), East China Sea (Cai et al., 2011), North Yellow Sea (Zhai et al., 2015), among others.

3.3. The buffering capacity of Guanabara Bay

The buffer factors calculated for the bay also presented spatio-temporal variabilities, following the same patterns described for the values of Ω_{arag}, as expected. The Fig. 8 presents the relationship between the buffers calculated in the bay against the E-DIC, AOU and TA/DIC ratio. The lowest values of E-DIC, AOU and TA/DIC were related to the highest buffer capacity in Guanabara and associated with phytoplankton blooms (the buffers were positively correlated to Chl *a* concentrations). The maximum values for the buffers γ_{DIC}, β_{DIC} and ω_{DIC} abs were 0.22 mmol kg^{-1}, 0.33 mmol kg^{-1} and 0.65 mmol kg^{-1}, respectively. As discussed by Hu et al. (2017), the high buffer capacity can be attributed to different reasons, including the high primary productivity and the warm waters. The lowest buffered waters were prevalent in sector 2, the most polluted region. In addition, as discussed above for the Ω_{arag} variations, Guanabara Bay showed significant vertical differences in the buffering capacity, with lower buffered bottom waters and higher buffered surface waters. This means that the microbial respiration at bottom waters can contributes to decrease the buffer capacity, decreasing the TA/DIC ratio. The marine carbonate system has a minimum buffering capacity when DIC equals to that of TA and with this condition any addition or removal of CO_2 will result in a maximum pH decrease or increase (Egleston et al., 2010). The Fig. 8 shows that the buffering capacity changes according to the specific buffer factors. However, the buffer factors have similar absolute values and similar qualitative behaviors (Egleston et al., 2010). Because these buffers change in a similar magnitude, the contribution to acidification or "basification" are largely related to physical (mixing) and biogeochemical processes (Cai et al., 2017).

A recent study conducted in the Cheasapeake Bay showed that the waters inside the bay were more vulnerable to anthropogenic and biological acidification due to the lower buffering capacity than offshore waters (Cai et al., 2017). For Guanabara Bay, however, we found an inverse trend. The intermediate waters of Guanabara Bay presented the highest buffering capacity because sector 3, the most productive region of the bay, presented higher aragonite saturation state than sector 1, closest to offshore waters. In this way, Guanabara Bay presented a behavior similar to that found in the Northern Gulf of Mexico, where the β_{DIC} spanned from 0.16 to 0.36 mmol kg^{-1} (Hu et al., 2017), very close to Guanabara Bay values ranging between 0.10 and 0.33 mmol kg^{-1}. These values are higher than for the entire global

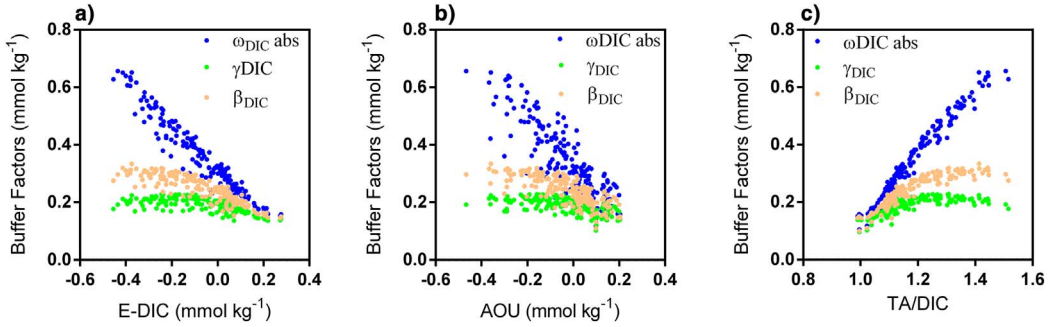

Fig. 8. Relationships between the buffer factors (β_{DIC}, γ_{DIC}, ω_{DIC}) and the concentrations of: a) E-DIC, b) AOU, c) TA/DIC, for all the data in Guanabara Bay.

surface ocean, which had a β_{DIC} range of 0.16–0.28 mmol kg^{-1} (Egleston et al., 2010; Hu et al., 2017). However, again, it must keep in mind that in Guanabara Bay the higher buffering capacity in surface waters can be counteracted by the lower buffering capacity in bottom waters and in the polluted sector 2.

4. Conclusions

Guanabara Bay showed a high spatio-temporal variability of Ω_{arag} related to the processes of production and respiration of organic matter that are intense due to the high eutrophication in the bay. The nutrient enrichment can amplify both production and respiration and can reduce or exacerbate the biological-induced acidification in coastal waters (Nixon et al., 2015) and this seems the case for Guanabara Bay. The highest values of Ω_{arag} were found at mid-upper surface waters, which are stratified, highly productive and dominated by phytoplankton blooms, with high buffering capacity. The lowest values of Ω_{arag} were found in well-mixed waters of the most polluted region of the bay that receives large amounts of effluent discharges, with strong heterotrophic activities and low buffering capacity, with episodic events of corrosive waters ($\Omega_{arag} < 1$). The lower values of Ω_{arag} at bottom waters compared to surface waters suggest a bottom acidification induced by microbial respiration during the settlement of autochthonous organic matter, especially at summer period. The eutrophication in Guanabara Bay is driving important environmental changes and acting to both increase or decrease the Ω_{arag} depending on the physical mixing and biogeochemical processes, despite the anthropogenic influence at the surroundings and watershed. In this sense, the biological metabolism in Guanabara Bay seems to be more important to produces changes in the aquatic carbonate chemistry than the changes related to the increase of atmospheric CO_2 concentrations.

Acknowledgments

This study was supported by the No Frontier Sciences Program of the Brazilian National Council of Research and Development (CNPq-Pve No 401.726/2012-6). Luiz C. Cotovicz Jr. is a postdoctoral researcher of the Carlos Chagas Foundation for Research Support of the State of Rio de Janeiro (FAPERJ; proc. no. E-26202.785/2016); B. A. Knoppers is a senior scientist of CNPq (proc. no. 301572/2010-0). We would like also to thank the FAPERJ Project Nr. E-26/111.190/2011 that contributed with the logistical support, and Dr. Xinping Hu (Texas A & M University) for the support to calculate the buffer factors.

References

Aberle, N., Schulz, K.G., Stuhr, A., Malzahn, A.M., Ludwig, A., Riebesell, U., 2013. High tolerance of microzooplankton to ocean acidification in an Arctic coastal plankton community. Biogeosciences 10, 1471–1481. http://dx.doi.org/10.5194/bg-10-1471-2013.

Abril, G., Frankignoulle, M., 2001. Nitrogen – alkalinity interactions in the highly polluted Scheldt Basin (Belgium). Water Res. 35, 844–850.

Abril, G., Etcheber, H., Delille, B., Frankignoulle, M., Borges, A.V., 2003. Carbonate dissolution in the turbid and eutrophic Loire estuary. Mar. Ecol. Prog. Ser. 259, 129–138.

Benson, B.B., Krause, D., 1984. The concentration and isotopic fractionation of oxygen dissolved in freshwater and seawater in equilibrium with the atmosphere. Limnol. Oceanogr. 29, 620–632.

Biswas, H., Gadi, S.D., Ramana, V.V., Bharathi, M.D., Priyan, R.K., Manjari, D.T., Kumar, M.D., 2012. Enhanced abundance of tintinnids under elevated CO_2 level from coastal Bay of Bengal. Biodivers. Conserv. 21, 1309–1326. http://dx.doi.org/10.1007/s10531-011-0209-7.

Boltovskoy, E., Scott, D.B., Medioli, F.S., 1991. Morphological variations of benthic foraminiferal tests in response to changes in ecological parameters: a review. J. Paleontol. 65, 175–184. http://dx.doi.org/10.1017/S0022336000020394.

Borges, A.V., Abril, G., 2011. Carbon dioxide and methane dynamics in estuaries. In: Eric, W., Donald, M. (Eds.), Treatise on Estuarine and Coastal Science. Academic Press, Amsterdam, pp. 119–161.

Borges, A.V., Gypens, N., 2010. Carbonate chemistry in the coastal zone responds more strongly to eutrophication than to ocean acidification. Limnol. Oceanogr. 55, 346e353.

Bricker, S.B., Ferreira, J.G., Simas, T., 2003. An integrated methodology for assessment of estuarine trophic status. Ecol. Model. 169, 39–60.

Cai, W.-J., Hu, X., Huang, W., Murrell, M.C., Lehrter, J.C., Lohrenz, S.E., Chou, W., Zhai, W., Hollibaugh, J.T., Wang, Y., Zhao, P., Guo, X., Gundersen, K., Dai, M., Gong, G., 2011. Acidification of Subsurface Coastal Waters Enhanced by Eutrophication. 4http://dx.doi.org/10.1038/NGEO1297.

Cai, W.-J., Huang, W.-J., Luther, G.W., Pierrot, D., Li, M., Testa, J., Xue, M., Joesoef, A., Mann, R., Brodeur, J., Xu, Y.-Y., Chen, B., Hussain, N., Waldbusser, G.G., Cornwell, J., Kemp, W.M., 2017. Redox reactions and weak buffering capacity lead to acidification in the Chesapeake Bay. Nat. Commun. 8, 369. http://dx.doi.org/10.1038/s41467-017-00417-7.

Cantoni, C., Luchetta, A., Celio, M., Cozzi, S., Raicich, F., Catalano, G., 2012. Carbonate system variability in the Gulf of Trieste (North Adriatic Sea). Estuar. Coast. Shelf Sci. 115, 51–62. http://dx.doi.org/10.1016/j.ecss.2012.07.006.

Carreira, R.S., Wagener, A.L.R., Readman, J.W., Fileman, T.W., Macko, S.a., Veiga, Á., 2002. Changes in the sedimentary organic carbon pool of a fertilized tropical estuary, Guanabara Bay, Brazil: an elemental, isotopic and molecular marker approach. Mar. Chem. 79, 207–227. http://dx.doi.org/10.1016/S0304-4203(02)00065-8.

Chou, W.C., Gong, G.C., Hung, C.C., Wu, Y.H., 2013. Carbonate mineral saturation states in the East China Sea: present conditions and future scenarios. Biogeosciences 10, 6453–6467. http://dx.doi.org/10.5194/bg-10-6453-2013.

Clemente, I.M.M.M., Silva, F.S., Laut, L.L.M., Frontalini, F., da Costa, V.L., Rodrigues, M.A., Pereira, E., Bergamaschi, S., Mendonça Filho, J.G., Martins, M.V.A., 2014. Biochemical composition and foraminiferal content of sediments for determining bottom sector environments in Guanabara Bay (Rio de Janeiro, Brazil). J. Coast. Res. 315, 1190–1204. http://dx.doi.org/10.2112/JCOASTRES-D-14-00104.1.

Cotovicz Jr., L.C., Knoppers, B.A., Brandini, N., Costa Santos, S.J., Abril, G., 2015. A strong CO_2 sink enhanced by eutrophication in a tropical coastal embayment (Guanabara Bay, Rio de Janeiro, Brazil). Biogeosciences 12, 6125–6146. http://dx.doi.org/10.5194/bg-12-6125-2015.

Cotovicz, L.C., Knoppers, B.A., Brandini, N., Poirier, D., Costa Santos, S.J., Abril, G., 2016. Spatio-temporal variability of methane (CH_4) concentrations and diffusive fluxes from a tropical coastal embayment surrounded by a large urban area (Guanabara Bay, Rio de Janeiro, Brazil). Limnol. Oceanogr. 61, S238–S252. http://dx.doi.org/10.1002/lno.10298.

Dejong, H.B., Dunbar, R.B., Mucciarone, D., Koweek, D.A., 2015. Carbonate saturation state of surface waters in the Ross Sea and Southern Ocean: controls and implications for the onset of aragonite undersaturation. Biogeosciences 12, 6881–6896. http://dx.doi.org/10.5194/bg-12-6881-2015.

Diaz, R.J., Rosenberg, R., 2008. Spreading dead zones and consequences for marine ecosystems. Science 321, 926–929.

Dickson, A.G., 1990. Thermodynamics of the dissociation of boric acid in synthetic seawater from 273.15 to 318.15 K. Deep-Sea Res. I Oceanogr. Res. Pap. 37, 755–766.

Dickson, A.G., 2010. The carbon dioxide system in seawater: equilibrium chemistry and measurements. In: Riebesell, U., Fabry, V.J., Hansson, L., Gattuso, J.-P. (Eds.), Guide to Best Practices for Ocean Acidification Research and Data Reporting. Publications Office of the European Union, Luxembourg, pp. 17–40.

Dickson, A.G., Millero, F.J., 1987. A comparison of the equilibrium constants for the dissociation of carbonic acid in seawater media. Deep-Sea Res. 34, 1733–1743.

Doney, S.C., Fabry, V.J., Feely, R., Kleypas, J.A., 2009. Ocean acidification: the other CO_2 problem. Annu. Rev. Mar. Sci. 1, 169–192. http://dx.doi.org/10.1146/annurev.marine.010908.163834.

Duarte, C.M., Hendriks, I.E., Moore, T.S., Olsen, Y.S., Steckbauer, A., Ramajo, L., Carstensen, J., Trotter, J.a., McCulloch, M., 2013. Is ocean acidification an open-ocean syndrome? Understanding anthropogenic impacts on seawater pH. Estuar. Coasts 36, 221–236. http://dx.doi.org/10.1007/s12237-013-9594-3.

Egleston, E.S., Sabine, C.L., Morel, F.M.M., 2010. Revelle revisited: buffer factors that quantify the response of ocean chemistry to changes in DIC and alkalinity. Glob. Biogeochem. Cycles 24, 1–9. http://dx.doi.org/10.1029/2008GB003407.

Feely, R. a, Sabine, C.L., Hernandez-Ayon, J.M., Ianson, D., Hales, B., 2008. Evidence for upwelling of corrosive "acidified" water onto the continental shelf. Science 320, 1490–1492. http://dx.doi.org/10.1126/science.1155676.

Feely, R.A., Alin, S.R., Newton, J., Sabine, S.L., Warner, M., Devol, A., Krembs, C., Maloy, C., 2010. The combined effects of ocean acidification, mixing, and respiration on pH and carbonate saturation in an urbanized estuary. Estuar. Coast. Shelf Sci. 88, 442e449.

Ferreira, J.G., Andersen, J.H., Borja, A., Bricker, S.B., Camp, J., Cardoso da Silva, M., Garcés, E., Heiskanen, A.-S., Humborg, C., Ignatiades, L., Lancelot, C., Menesguen, A., Tett, P., Hoepffner, N., Claussen, U., 2011. Overview of eutrophication indicators to assess environmental status within the European Marine Strategy Framework Directive. Estuar. Coast. Shelf Sci. http://dx.doi.org/10.1016/j.ecss.2011.03.014.

Fistarol, G.O., Coutinho, F.H., Moreira, A.P.B., Venas, T., Cánovas, A., de Paula, S.E.M., Coutinho, R., de Moura, R.L., Valentin, J.L., Tenenbaum, D.R., Paranhos, R., do Valle, R.D.A.B., Vicente, A.C.P., Amado Filho, G.M., Pereira, R.C., Kruger, R., Rezende, C.E., Thompson, C.C., Salomon, P.S., Thompson, F.L., 2015. Environmental and sanitary conditions of Guanabara Bay, Rio de Janeiro. Front. Microbiol. 6, 1232. http://dx.doi.org/10.3389/fmicb.2015.01232.

Fitzer, S.C., Chung, P., Maccherozzi, F., Dhesi, S.S., Kamenos, N.A., Phoenix, V.R., Cusack, M., 2016. Biomineral shell formation under ocean acidification: a shift from order to chaos. Sci Rep 6, 21076. http://dx.doi.org/10.1038/srep21076.

Frankignoulle, M., 1994. A complete set of buffer factors for acid/base CO_2 system in seawater. J. Mar. Syst. 5, 111–118.

Frankignoulle, M., Borges, A., Biondo, R., 2001. A new design of equilibrator to monitor carbon dioxide in highly dynamic and turbid environments. Water Res. 35, 1344–1347.

Gattuso, J.-P., Magnan, A., Billé, R., Cheung, W.W.L., Howes, E.L., Joos, F., Allemand, D.,

Bopp, L., Cooley, S.R., Eakin, C.M., Hoegh-Guldberg, O., Kelly, R.P., Pörtner, H.-O., Rogers, A.D., Baxter, J.M., Laffoley, D., Osborn, D., Rankovic, A., Rochette, J., Sumaila, U.R., Treyer, S., Turley, C., 2015. Oceanography. Contrasting futures for ocean and society from different anthropogenic CO_2 emissions scenarios. Science 349, aac4722. http://dx.doi.org/10.1126/science.aac4722.

Godoy, J.M., Oliveira, A.O., Almeida, A.C., Godoy, M.L., Moreira, I., Wagener, A.R., Figueiredo Junior, A.G., 2012. Guanabara Bay sedimentation rates based on 210Pb dating: reviewing the existing data and adding new data. J. Braz. Chem. Soc. 23, 1265–1273.

Gran, G., 1952. Determination of the equivalence point in potentiometric titrations-part II. Analyst 77, 661–671.

Howarth, R., Chan, F., Conley, D.J., Garnier, J., Doney, S.C., Marino, R., Billen, G., 2011. Coupled biogeochemical cycles: eutrophication and hypoxia in temperate estuaries and coastal marine ecosystems. Front. Ecol. Environ. 9, 18–26. http://dx.doi.org/10.1890/100008.

Hu, X., Cai, W.-J., 2011. An assessment of ocean margin anaerobic processes on oceanic alkalinity budget. Glob. Biogeochem. Cycles 25, n/a. http://dx.doi.org/10.1029/2010GB003859.

Hu, X., Li, Q., Huang, W.J., Chen, B., Cai, W.J., Rabalais, N.N., Eugene Turner, R., 2017. Effects of eutrophication and benthic respiration on water column carbonate chemistry in a traditional hypoxic zone in the Northern Gulf of Mexico. Mar. Chem. 194, 33–42. http://dx.doi.org/10.1016/j.marchem.2017.04.004.

Huang, W.-J., Cai, W.-J., Powell, R.T., Lohrenz, S.E., Wang, Y., Jiang, L.-Q., Hopkinson, C.S., 2012. The stoichiometry of inorganic carbon and nutrient removal in\newline the Mississippi River plume and adjacent continental shelf. Biogeosciences 9, 2781–2792. http://dx.doi.org/10.5194/bg-9-2781-2012.

IPCC, 2013. In: T. F. Stocker, et al. (Ed.), Climate Change 2013: The Physical Science Basis. Contribution of Working Group I to the Fifth Assessment Report of the Intergovernmental Panel on Climate Change. Cambridge Univ. Press. http://dx.doi.org/10.1017/CBO9781107415324.

Jiang, L.-Q., Cai, W.-J., Wang, Y., Bauer, J.E., 2013. Influence of terrestrial inputs on continental shelf carbon dioxide. Biogeosciences 10, 839–849. http://dx.doi.org/10.5194/bg-10-839-2013.

Kalas, F.A., Carreira, R.S., Macko, S.A., Wagener, A.L.R., 2009. Molecular and isotopic characterization of the particulate organic matter from an eutrophic coastal bay in SE Brazil. Cont. Shelf Res. 29, 2293–2302. http://dx.doi.org/10.1016/j.csr.2009.09.007.

Kjerfve, B., Ribeiro, C.H.A., Dias, G.T.M., Filippo, A.M., Da Silva Quaresma, V., 1997. Oceanographic characteristics of an impacted coastal bay: Baía de Guanabara, Rio de Janeiro, Brazil. Cont. Shelf Res. 17, 1609–1643. http://dx.doi.org/10.1016/S0278-4343(97)00028-9.

Kroeker, K.J., Kordas, R.L., Crim, R.N., Singh, G.G., 2010. Meta-analysis reveals negative yet variable effects of ocean acidification on marine organisms. Ecol. Lett. 13, 1419–1434. http://dx.doi.org/10.1111/j.1461-0248.2010.01518.x.

Kubo, A., Maeda, Y., Kanda, J., 2017. A significant net sink for CO_2 in Tokyo Bay. Sci Rep 7, 44355. http://dx.doi.org/10.1038/srep44355.

Le Quéré, C., Andrew, R.M., Canadell, J.G., Sitch, S., Ivar Korsbakken, J., Peters, G.P., Manning, A.C., Boden, T.A., Tans, P.P., Houghton, R.A., Keeling, R.F., Alin, S., Andrews, O.D., Anthoni, P., Barbero, L., Bopp, L., Chevallier, F., Chini, L.P., Ciais, P., Currie, K., Delire, C., Doney, S.C., Friedlingstein, P., Gkritzalis, T., Harris, I., Hauck, J., Haverd, V., Hoppema, M., Klein Goldewijk, K., Jain, A.K., Kato, E., Körtzinger, A., Landschützer, P., Lefèvre, N., Lenton, A., Lienert, S., Lombardozzi, D., Melton, J.R., Metzl, N., Millero, F., Monteiro, P.M.S., Munro, D.R., Nabel, J.E.M.S., Nakaoka, S.I., O'Brien, K., Olsen, A., Omar, A.M., Ono, T., Pierrot, D., Poulter, B., Rödenbeck, C., Salisbury, J., Schuster, U., Schwinger, J., Séférian, R., Skjelvan, I., Stocker, B.D., Sutton, A.J., Takahashi, T., Tian, H., Tilbrook, B., Van Der Laan-Luijkx, I.T., Van Der Werf, G.R., Viovy, N., Walker, A.P., Wiltshire, A.J., Zaehle, S., 2016. Global carbon budget 2016. Earth Syst. Sci. Data 8, 605–649. http://dx.doi.org/10.5194/essd-8-605-2016.

Lee, K., Kim, T.W., Byrne, R.H., Millero, F.J., Feely, R.A., Liu, Y.M., 2010. The universal ratio of boron to chlorinity for the North Pacific and North Atlantic oceans. Geochim. Cosmochim. Acta 74, 1801–1811.

Mathis, J.T., Cross, J.N., Bates, N.R., Bradley Moran, S., Lomas, M.W., Mordy, C.W., Stabeno, P.J., 2010. Seasonal distribution of dissolved inorganic carbon and net community production on the Bering Sea shelf. Biogeosciences 7, 1769–1787. http://dx.doi.org/10.5194/bg-7-1769-2010.

Mehrbach, C., Culberson, C.H., Hawley, J.E., Pytkowicz, R.M., 1973. Measurements of the apparent dissociation constants of carbonic acid in seawater at atmospheric pressure. Limnol. Oceanogr. 18, 897–907.

Meniconi, M.F.G., Silva, T.A., Fonseca, M.L., Lima, S.O.F., Lima, E.F.A., Lavrado, H.P., Figueiredo Jr., A.G., 2012. Baia de Guanabara: síntese do conhecimento ambiental. Vol. 2 PETROBRAS, Rio de Janeiro.

Miles, H., Widdicombe, S., Spicer, J.I., Hall-Spencer, J., 2007. Effects of anthropogenic seawater acidification on acid-base balance in the sea urchin *Psammechinus miliaris*. Mar. Pollut. Bull. 54, 89–96. http://dx.doi.org/10.1016/j.marpolbul.2006.09.021.

Millero, F.J., 1979. The thermodynamics of the carbonate system in seawater. Geochim. Cosmochim. Acta 43, 1651–1661.

Millero, F.J., 2007. The marine inorganic carbon cycle. Chem. Rev. 107, 308–341. http://dx.doi.org/10.1021/cr0503557.

Morse, J.W., Arvidson, R.S., Lüttge, A., 2007. Calcium carbonate formation and dissolution. Chem. Rev. 107, 342–381. http://dx.doi.org/10.1021/cr050358j.

Mucci, A., 1983. The solubility of calcite and aragonite in seawater at various salinities, temperatures, and one atmosphere total pressure. Am. J. Sci. 283, 780e799.

Murray, J.W., 2006. Ecology and Applications of Benthic Foraminifera. Cambridge University Press, Cambridge, United Kingdom (426p).

Nixon, S.W., 1995. Coastal marine eutrophication: a definition, social causes, and future concerns. Ophelia 41, 199–219.

Nixon, S.W., Oczkowski, A.J., Pilson, M.E.Q., Fields, L., Oviatt, C.A., Hunt, C.W., 2015. On the response of pH to inorganic nutrient enrichment in well-mixed coastal marine waters. Estuar. Coasts 38, 232–241. http://dx.doi.org/10.1007/s12237-014-9805-6.

Provoost, P., van Heuven, S., Soetaert, K., Laane, R.W.P.M., Middelburg, J.J., 2010. Seasonal and long-term changes in pH in the Dutch coastal zone. Biogeosciences 7, 3869–3878. http://dx.doi.org/10.5194/bg-7-3869-2010.

Rabalais, N.N., Turner, R.E., Diaz, R.J., Justic, D., 2009. Global change and eutrophication of coastal waters. ICES J. Mar. Sci. 66, 1528–1537. http://dx.doi.org/10.1093/icesjms/fsp047.

Rebello, A.L., Ponciano, C.R., Melges, L.H., 1988. Avaliação da produtividade primaria e da disponibilidade de nutrientes na Baia de Guanabara. An. Acad. Bras. Cienc. 419–430 (1988), 60.

Ribeiro, C., Kjerfve, B., 2002. Anthropogenic influence on the water quality in Guanabara Bay, Rio de Janeiro, Brazil. Reg. Environ. Chang. 3, 13–19. http://dx.doi.org/10.1007/s10113-001-0037-5.

Robbins, L.L., Hansen, M.E., Kleypas, J.A., 2010. CO2 Calc: a user-friendly seawater carbon calculator for Windows, Max OS X, and iOS (iPhone). U.S. Geological Survey Open-File Report, 2010–1280. pp. 1–17. available at: http://pubs.usgs.gov/of/2010/1280/ (last access: 6 January 2016).

Salisbury, J., Green, M., Hunt, C., Campbell, J., 2008. Coastal acidification by rivers: a threat to shellfish? Eos (Washington DC) 89, 513. http://dx.doi.org/10.1029/2008EO500001.

Santos, V.S., Villac, M.C., Tenenbaum, D.R., 2007. Auto- and heterotrophic nanoplankton and filamentous bacteria of Guanabara Bay (RJ, Brazil): estimates of cell/filament numbers versus carbon content. Braz. J. Oceanogr. 55, 133–143.

Strickland, J.D.H., Parsons, T.R., 1972. A Practical Handbook of Seawater Analysis, second ed. Fisheries Research Board of Canada Bulletin, Ottawa, Canada.

Sunda, W.G., Cai, W.-J., 2012. Eutrophication induced CO_2-acidification of subsurface coastal waters: interactive effects of temperature, salinity, and atmospheric P(CO(2)). Environ. Sci. Technol. 46, 10651–10659. http://dx.doi.org/10.1021/es300626f.

Valentin, J.L., Tenembaum, D.R., Bonecker, A.C.T., Bonecker, S.L.C., Nogeuira, C.L., Villac, M.C., 1999. O sistema planctônico da Baia de Guanabara: síntese do conhecimento. Ecologia dos ambientes costeiros do Estado do Rio de Janeiro. Series Oecologia Brasiliensis PPg-UFRJ, Rio de Janeiro, Brazil VII, pp. 35–59.

Vilela, C.G., Sanjines, A., Ghiselli, R.J., Filho, J., Neto, J., Barbosa, C.F., 2003. Search for bioindicators of pollution in the Guanabara Bay: integrations of ecologic patterns. Anu. Inst. Geocienc. 26, 25–35.

Villac, M.C., Tenenbaum, D.R., 2010. The phytoplankton of Guanabara Bay, Brazil. I. Historical account of its biodiversity. Biota Neotrop. 10, 271–293.

Wallace, R.B., Baumann, H., Grear, J.S., Aller, R.C., Gobler, C.J., 2014. Coastal ocean acidification: the other eutrophication problem. Estuar. Coast. Shelf Sci. 148, 1–13. http://dx.doi.org/10.1016/j.ecss.2014.05.027.

Wang, Z.A., Kroeger, K.D., Ganju, N.K., Gonneea, M.E., Chu, S.N., 2016. Intertidal salt marshes as an important source of inorganic carbon to the coastal ocean. Limnol. Oceanogr. 61, 1916–1931. http://dx.doi.org/10.1002/lno.10347.

Weiss, R.F., 1974. Carbon dioxide in water and seawater: the solubility of a non-ideal gas. Mar. Chem. 2, 203–215.

Winde, V., Böttcher, M.E., Escher, P., Böning, P., Beck, M., Liebezeit, G., Schneider, B., 2014. Tidal and spatial variations of DI13C and aquatic chemistry in a temperate tidal basin during winter time. J. Mar. Syst. 129, 396–404. http://dx.doi.org/10.1016/j.jmarsys.2013.08.005.

Xue, L., Cai, W.-J., Hu, X., Sabine, C., Jones, S., Sutton, A.J., Jiang, L.-Q., Reimer, J.J., 2016. Sea surface carbon dioxide at the Georgia time series site (2006–2007): air–sea flux and controlling processes. Prog. Oceanogr. 140, 14–26. http://dx.doi.org/10.1016/j.pocean.2015.09.008.

Xue, L., Cai, W.-J., Sutton, A.J., Sabine, C., 2017. Sea surface aragonite saturation state variations and control mechanisms at the Gray's Reef time-series site off Georgia, USA (2006–2007). Mar. Chem. http://dx.doi.org/10.1016/j.marchem.2017.05.009.

Zhai, W., Dai, M., Guo, X., 2007. Carbonate system and CO_2 degassing fluxes in the inner estuary of Changjiang (Yangtze) River, China. Mar. Chem. 107, 342–356. http://dx.doi.org/10.1016/j.marchem.2007.02.011.

Zhai, W.D., Zang, K.P., Huo, C., Zheng, N., Xu, X.M., 2015. Occurrence of aragonite corrosive water in the North Yellow Sea, near the Yalu River estuary, during a summer flood. Estuar. Coast. Shelf Sci. 166, 199–208. http://dx.doi.org/10.1016/j.ecss.2015.02.010.

Zhang, J.-Z., Fischer, C.J., 2014. Carbon dynamics of Florida Bay: spatiotemporal patterns and biological control. Environ. Sci. Technol. 48, 9161–9169. http://dx.doi.org/10.1021/es500510z.

Zhang, L., Xue, M., Liu, Q., 2012. Distribution and seasonal variation in the partial pressure of CO_2 during autumn and winter in Jiaozhou Bay, a region of high urbanization. Mar. Pollut. Bull. 64, 56–65. http://dx.doi.org/10.1016/j.marpolbul.2011.10.023.